2009 American Control Conference
Hyatt Regency Riverfront, St. Louis, MO, USA
June 10-12, 2009

LQG-based tracking of multiple fluorescent particles in two-dimensions in a confocal microscope

Zhaolong Shen and Sean B. Andersson

***Abstract*— This paper describes a scheme to track multiple fluorescent particles diffusing in two dimensions. Fluorescence intensities are measured using a scanning-stage confocal setup. We develop a combined model for the position of the particles and the dynamics of the piezo-stage and design a linear-quadratic-Gaussian controller to drive the overall estimation error to zero. The scheme is illustrated through simulation.**

I. Introduction

Particle tracking is an important class of tools for studying single-molecule systems in molecular biology. Based on the number of particles to track, algorithms can be divided into two main categories: single particle tracking (SPT) and multiple particle tracking (MPT). SPT has been used in the study of many systems and has been shown useful in measuring diffusion coefficients [1], in discriminating molecules according to their mobility [2] and in revealing dynamics of signaling receptors [3]. Most approaches rely on wide-field imaging using CCD cameras followed by image processing. The temporal resolution is limited by the speed and sensitivity of the CCD imagers to at best a few millseconds for two-dimensional studies and to hundreds of milliseconds to seconds for three-dimensional studies. These slow times severely restrict the systems that can be investigated with these techniques.

The temporal resolution can be improved by orders-of-magnitude by using single photon counters and confocal (or multi-photon) setups instead of CCD cameras in a wide-field setup. Particle tracking in this setting is achieved by actuating the detection volume relative to the particle. Most work to date is targeted at SPT [4]–[7]. The general approach in most of these efforts is to move the detection volume rapidly in a circular pattern and to use the measured fluorescence intensity to estimate the position of the particle. This has been combined this scheme is coupled to a linear quadratic Gaussian (LQG) controller to achieve tracking of a single particle in two dimensions [4] and in three dimensions [8].

The goal of MPT is to provide the trajectories of multiple particles simultaneously. This is critical in revealing overall bulk transport properties and the properties of the environment itself. MPT has been used to measure heterogeneities in solutions of actin filaments and actin bundles [9] and has found application in drug and gene delivery [10]. Most MPT methods rely on image processing of wide-field images. As with SPT, the time and spatial resolution are limited by the CCD imagers. Moreover, it is time consuming to extract the position information from images and the results are sensitive to background noise. To date, there has been relatively little work on MPT in the confocal setup, although [6] did apply a single particle tracking scheme to multiple particles by simply cycling between the particles.

In this paper, we take an approach similar to [4], here extending the scheme to N particles. The result is an LQG controller designed to track particles moving under Brownian diffusion in two dimensions in a confocal microscope. Unlike [4], however, we do not drive the detection volume rapidly around a circular pattern to obtain a position estimate. Rather we obtain a small number of measurements near to the current estimate and use an estimation algorithm developed by one of the authors [11]. This algorithm needs only measurements of the fluorescence intensity at as few as three different locations around the particle. As a result, it does not require high speed beam steering. The overall tracking scheme is therefore easier to implement.

II. System model

In this section we develop the complete system model for both the single particle and multiple particle settings. A block diagram of the approach is shown in Fig. 1

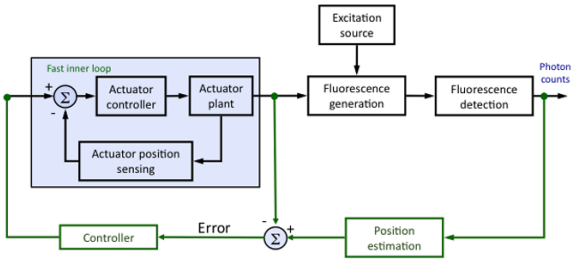

Fig. 1. Block diagram for single particle tracking. An LQG-based controller is implemented to achieve particle tracking. In the multiple particle case, a collection of such systems is switched between.

A. Actuator models

Although the work in this paper utilizes simulations to explore the algorithm, it is our intent to implement the algorithm on a home-built confocal microscope in our lab. Thus the system model is based on a nano-positioning stage built into the microscope (a Mad City Labs Nano-PDQ). The nanostage can be run either in closed loop mode, in which a controller provided by the manufacturer is used to drive the actuators, or in open-loop mode in which the commands are simply amplified and applied to the piezos. We identified the transfer function for both modes and then designed our

Both authors are with the Dept. of Mech. Eng., Boston University, Boston, MA, 02215, USA.
{zlshen,sanderss}@bu.edu

own controller to improve the positioning dynamics. By simulating with both the built-in controller and our higher-performance controller, we can obtain information on the effect of the stage dynamics on the tracking scheme.

Fig. 2 shows the closed-loop Bode plots of the x-axis of the stage under the built-in controller and under our controller. The closed-loop cutoff frequency is improved from approximately 300 Hz (built-in) to 2 kHz (our controller).

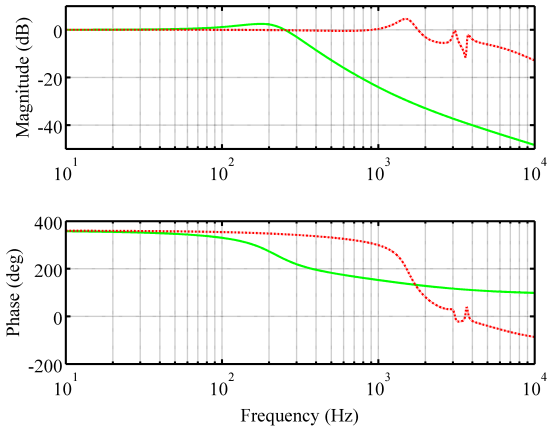

Fig. 2. Close loop Bode plots of stage under two different feedback controllers. The solid red curve is the built-in controller provided by the manufacturer and the dashed blue curve is our controller.

B. Single particle model and position estimation

We assume the two axes are independent and first derive the system model for the $x-$axis. Let the dynamics of the translation stage be given by the transfer function $G_x(s)$

$$G_x(s) = \frac{X_s(s)}{U_x(s)} \tag{1}$$

where x_s represents the position of the stage and u_x represents the input voltage to the $x-$axis piezo.

The Brownian motion of a particle in one dimension is described by the stochastic differential equation

$$dx_p(t) = \sqrt{2D}dw_x(t) \tag{2}$$

where x_p is the position of particle, D its diffusion coefficient, and $dw_x(t)$ an infinitesimal Wiener increment with mean 0 and variance dt where dt is sampling time of system. We take as the system state

$$X = [x_p\ x_s\ \dot{x}_s \cdots x_s^{(n-1)}\ u_x\ \dot{u}_x \cdots u_x^{(m-1)}]^T \tag{3}$$

and as control input the highest relevant time-derivative of the driving voltage of stage $u_x(t)$:

$$u(t) = \frac{d^m}{dt^m}u_x(t). \tag{4}$$

The system output is modeled as the difference between the location of the particle and the position of the stage plus measurement noise:

$$y_x(t) = x_p(t) - x_s(t) + v_x(t). \tag{5}$$

This measurement is described in Sec. II-B.1 below.

The linear stochastic dynamic system for the $x-$axis in state-space can be written as,

$$\dot{X} = A_xX + B_xU_x + w_x,\ Y = C_xX + v_x, \tag{6}$$

where the matrices are derived from the transfer function. Since w_x comes from the Brownian motion of the particle, we have

$$W_x = E\left[w_xw_x^T\right] = \langle x_p^2\rangle = 2Ddt. \tag{7}$$

Noise in the measurements is driven primarily by autofluorescence in the sample and electronic (shot) noise in the sensors. These noises are filtered through the position estimation scheme described below. For the purposes of the system model, we assume the measurement noise v_x has a known covariance (determined through experiment) of

$$V_x = E\left[v_xv_x^T\right].$$

The $y-$axis can be modeled in the same manner as the $x-$axis. Thus the system model for tracking a single particle in two dimensions is given by appending a second single axis to the first. Note that the dynamics of the translation stage, $G_y(s)$ need not be the same as for the x-axis. The corresponding model is then

$$\dot{X} = A_oX + B_oU + w,\ Y = C_oX + v, \tag{8}$$

where

$$A_o = \begin{bmatrix} A_x & 0 \\ 0 & A_y \end{bmatrix},\ B_o = \begin{bmatrix} B_x & 0 \\ 0 & B_y \end{bmatrix},\ C_o = \begin{bmatrix} C_x & 0 \\ 0 & C_y \end{bmatrix},$$

$$w = \begin{bmatrix} w_x \\ w_y \end{bmatrix},\ v = \begin{bmatrix} v_x \\ v_y \end{bmatrix}.$$

1) Position estimation : To estimate the position of the particle, the fluoroBancroft algorithm [12] is used. This is an analytical formula that converts a set of at least three fluroescence intensity measurements taken at different positions in the plane into an estimate of the position of the particle. In this work, we obtain m intensity measurements as follows. For each actuator voltage u_x and u_y calculated by the controller (described in Section III below), we generate m additional scan voltages that are cycled through in series. These voltages drive the system through m points and at each of these we record both the fluorescence intensity and the position of the stage. These data are then used in the estimation algorithm to determine the position of the particle.

As more measurements are used in the estimation algorithm, the accuracy is improved at the cost of a larger total measurement time. During this time, the particle continues to move. This motion is not captured by the model and leads to increased estimation error.

C. Multiple particles model

Suppose now that there are N particles and N independent translation stages with which to track them. We can set up a state-space equation for this system by expanding the state-space model for the single particle tracking case to N copies:

$$\dot{X} = AX + BU + W,\ Y = CX + V, \tag{9}$$

where

$$A = \mathrm{diag}\{\overbrace{A_o, ..., A_o}^{N}\},\ B = \mathrm{diag}\{\overbrace{B_o, ..., B_o}^{N}\}$$
$$C = \mathrm{diag}\{\overbrace{C_o, ..., C_o}^{N}\}$$

In reality, there is only one translation stage. In this work, we simply cycle through each system in turn, tracking first particle one, then particle two, and so on. As a result, the sampling time on the full model is N times slower than the sampling time used on the translation stage. Optimizing both the cycling sequence and the relative amount of time spent on each particle remains an open problem.

Finally we note that in practice, the implementation will be done digitally and thus the above model is discretized based on the desired sampling time.

III. Tracking controller

In this section, we apply standard LQG controller design to achieve tracking. We initially consider the single particle model before moving to the multiple particle scenario.

A. Tracking a single particle

An LQG controller combines a Kalman filter for state estimation with a linear quadratic regulator (LQR) for control. Consider first the Kalman filter. Suppose the initial state of the particle model is a random variable with mean $\hat{X}_0$ and covariance Σ_0. One standard description of the discrete-time Kalman filter equations is given by the time update equations to produce the prediction $\hat{X}_{k+1|k}$ based on the model and the control input combined the measurement update equations to produce the estimate $\hat{X}_{k|k}$ from $\hat{X}_{k|k-1}$ and the innovations.

Consider now the LQR controller. For the $x-$axis, we define the cost function to be

$$J_x = \sum_{k=1}^{\infty} \lambda_x[(x_p(k) - x_s(k))^2 + \lambda_u u^2(k)] \tag{10}$$

where λ_x and λ_u are weights for the state and input. This cost defines the weighting matrices Q_x and R_x for the full state and input for the $x-$axis. A similar cost is defined for the $y-$axis. Then the cost matrix for one particle tracking system will be

$$Q_o = \mathrm{diag}\{Q_x, Q_y\},\ R_o = \mathrm{diag}\{R_x, R_y\}$$

such that the overall cost function is

$$J = J_x + J_y = X^T Q_o X + U^T R_o U. \tag{11}$$

The control that optimizes the quadratic cost is given by

$$U_k = -G_c \hat{X}_{k|k} \tag{12}$$

where the gain matrix G_c is

$$G_c = (R_o + B_o^T P_\infty B_o)^{-1} B_o^T P_\infty A_o. \tag{13}$$

Nominally, P_∞ would be the solution to the discrete-time algebraic Riccati equation (ARE). In our formulation, however, the position of the particle is driven purely by white noise and is not affected by control input. The system is thus uncontrollable and the ARE cannot be used. Instead, we use the steady-state solution to the Riccati equation

$$\begin{aligned} P_{k-1} &= Q_o + A_o P_k A_o^T \\ &\quad - A_o^T P_k B_o \left(R_o + B_o^T P_k B_o\right)^{-1} B_o^T P_k A_o \end{aligned}$$

since the components that diverge do not enter into the gain matrix G_o.

The control scheme for tracking a single particle is then as follows. Using the time update equations of the Kalman filter, we obtain the predicted state $\hat{X}(k+1|k)$. A component of this state is the predicted driving voltage (u_x, u_y) and the predicted stage position (x_s, y_s). Based on the driving voltage, the scan procedure described in the previous section is run and the particle position estimated from the fluorescence measurements. The state measurement is calculated as the difference between the estimated particle position and stage position. This output is then fed into the Kalman filter measurement update equations to generate $\hat{X}_{k+1|k+1}$.

B. Tracking multiple particles

The tracking scheme for multiple particles is to simply combine the LQG tracking controllers for each particle. The predicted driving voltages are determined from the LQG controller. The stage then simply cycles through the particles based on these voltages, running the estimation procedure on each. After all particles have been estimated, a single overall system measurement is generated, the Kalman filter updated, and the process repeated.

One of the primary differences between single and multiple particle tracking is the need for a relatively large shift in the acutators when moving between particles. Due to the actuator dynamics and depending on the sampling time of the system, overshoot or other transient effects may lead to poor positioning of the focal volume of the microscope. In extreme cases, this error may be large enough that the particle is not inside the focal volume at all, leading to loss of tracking. It is therefore important to design low-level controllers that yield small one-step positioning errors to improve tracking performance in the multiple particle case.

IV. Simulations

To explore the scheme and guide the selection of control parameters such as sampling frequency, number of measurements and the driving voltage scan radius, we performed a simulation study. Although in practice the dynamics of the actuation stage in the x and y directions can differ significantly, we set them equal here to focus on the effect of other control parameters. The stage transfer function corresponding to the manufacturer-provided closed-loop mode shown in Fig.2 was discretized using a sampling time of dt, while

in a simulation with N particles, the full system model is discretized with a sampling time of $Dt = Ndt$. The initial positions for each of the N particles positions were generated randomly and the stage position was initialized at the origin.

Fluorescence intensities were modeled according to [13]

$$I(x,y) = me^{-\frac{(x-x_p)^2+(y-y_p)^2}{\omega^2}} + \eta_B + \eta_S \qquad (14)$$

where m represents the maximum fluorescence value, ω the beam waist, η_B the background fluorescence, and η_S the shot noise. For these simulations, the beam waist was taken as $\omega = 0.5$ μm, the maximum intensity was given by a rate of 200,000 photon/s and the background fluorescence was given by a Poisson random variable with parameter set to 2000 photons/s. The measured intensity thus depended upon the sampling frequency. The shot noise was given by a Poisson random variable with parameter given by the total number of photons collected in the sampling period. Unless otherwise specified, position estimation was done based on five measurements, one at the predicted actuator position and four equally distributed on a circle of radius $u_r = 0.06$ V and centered on the predicted actuator position. Fig. 3 shows a single run for a particle diffusing with coefficient $D = 2$ μm^2/s. The solid blue curve is the (simulated) real particle position and the dotted red line is the estimated position based on the noisy measurement.

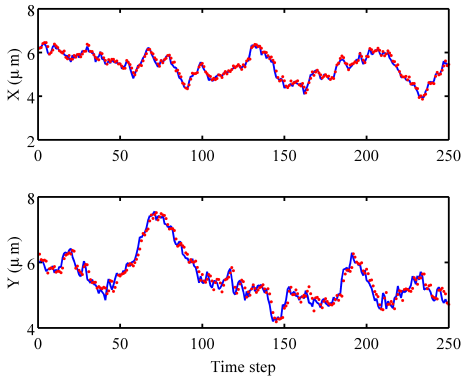

Fig. 3. Simulated single particle tracking performance. The particle is diffusing with a coefficient $D = 2$ μm^2/s (solid blue line). The dotted red line shows the estimated particle position from the Kalman filter.

A. Single particle tracking

1) Error as a function of diffusion coefficient: Fig. 4 shows the tracking error and the standard deviation in the error (error bars) as a function of the diffusion coefficient with a sampling rate of 250 Hz. Both the tracking error and its standard deviation increase as the diffusion coefficient is increased. Fundamentally, this error is driven by the motion of the particle during each time interval. Based on (7), the error and standard deviation should then be proportional to $\sqrt{D}$. This relationship holds roughly, with the mean and standard deviation approximately doubling as the diffusion constant in increased from 1 μm^2/s to 4 μm^2/s. After 4 μm^2/s the system was unable to maintain tracking since the particle diffused far enough away in one sample period so that it was not detected during the next estimation round.

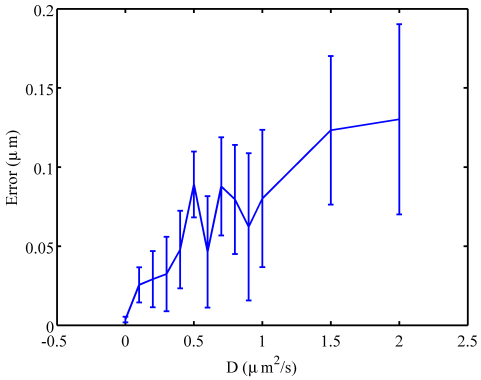

Fig. 4. Tracking error and std. dev. (error bars) as a function of the diffusion constant. The sampling frequency was fixed at 250 Hz. The error is driven by the diffusion of the particle during each measurement cycle and therefore grows roughly proportional to $\sqrt{D}$.

2) Error as a function of sampling frequency: Fig. 5 shows the tracking error and standard deviation for a fixed particle as a function of the sampling frequency. Because the particle is fixed, the error arises primarily from measurement noise. As the sampling frequency is increased, the measurement time for each measurement is decreased, leading to a poorer signal-to-noise ratio (SNR). This in turn leads to an increased tracking error.

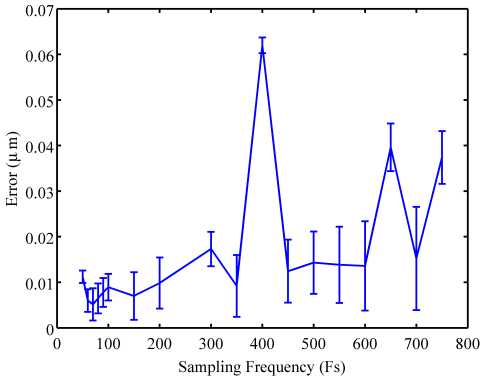

Fig. 5. Tracking error and std. dev. (error bars) as a function of the sampling frequency for a fixed particle. Increasing sampling frequency corresponds to decreasing SNR, leading to increased error in the position estimate. This in turn leads to poorer tracking performance.

When tracking a diffusing particle, additional error arises from the fact that the particle is constantly in motion. At low sampling frequencies, the SNR in the measurements is relatively high and the error due to the motion of the particle is dominant. Increasing the sampling frequency leads to a faster response by the controller and thus a decreased error. As the frequency is taken even higher, the SNR continues to decrease and the measurement noise plays a more dominant role. This is illustrated in Fig. 6(a) in which we show

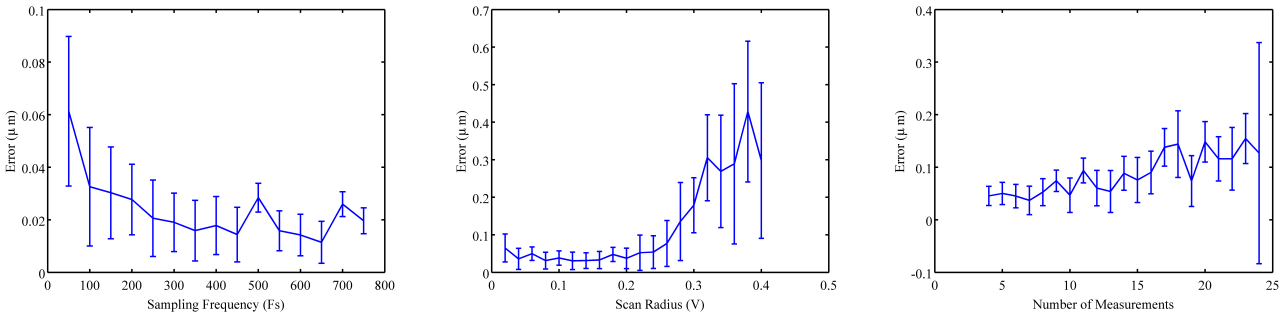

(a) Sampling frequency (b) Scan radius (c) Num. measurements

Fig. 6. Tracking error and std. dev. (error bars) as a function of different parameters for a particle diffusing with $D = 0.5$ μm^2/s. **(a)** At low sampling frequencies, the error due to particle motion dominates. Performance improves with increasing sampling frequency, eventually plateauing due to reduced SNR in the measurements. **(b)** Increasing the scan radius eventually leads to a reduced SNR that leads to a larger error. **(c)** increasing the number of measurements initially improves performance due to better position estimation. Increasing the number of measurements also increases the total measurement time, eventually leading to poorer performance due to motion of the particle during the measurement process.

the tracking error and standard deviation as a function of sampling frequency when tracking a diffusing particle with $D = 0.1$ μm^2/s. Tracking performance improves rapidly as the sampling frequency is increased to 300 Hz. After that the performance remains relatively constant, implying that the improvement in tracking due to a faster system response is offset by the corresponding reduction in the SNR.

3) Error as a function of scan radius: As described in Sec. II-B.1, position estimation is done based on a collection of samples obtained around a circle of radius u_r. If this radius is too large relative to the size of the beam waist, then the SNR will be low and position estimation will be poor. If the radius is too small then the measurement locations will be close together and this also yields poorer position estimation since each measurement provides essentially the same information. Moreover, for a small radius the region explored by the scanning procedure will be small. In this case, even at relatively small values of the diffusion constant, the particle will diffuse out of the region during the sample period, leading to a loss of tracking. These tradeoffs are exhibited in Fig. 6(b) in which we show the tracking error and standard deviation as a function of the scan radius when tracking a single particle moving with $D = 0.1$ μm^2/s. The sampling frequency was set to 250 Hz. For the simulated conditions, tracking performance was best for scan radii of 0.08 V to 0.15 V.

4) Error as a function of the number of measurements: Performance of the algorithm also depends on the number of measurements used in the estimation scheme. For a fixed particle, increasing the number of measurements leads to improved performance of the estimator at the cost of increased measurement time. For a diffusing particle, this increased measurement time leads to increased error due to the fact that the particle is constantly moving. In Fig. 6(c) we show the tracking error and standard deviation as a function of the number of measurements used in the estimation procedure. The sampling frequency was set to 250 Hz and the particle was diffusing with $D = 0.1$ μm^2/s. Tracking performance improved slightly as the number of measurements was increased from four to seven. Additional measurements yielded increasingly poorer performance. Tracking failed completely when more than 24 measurements were used in the estimation procedure.

B. Multiple particle tracking

For the multiple particle scenario, we fixed the sampling frequency to 500 Hz, the scan radius to 0.06 V, and the number of measurements used on each particle to five. In Fig. 7 (top) we show the tracking error and standard deviation when tracking two particles as a function of the diffusion coefficient. The maximum diffusion coefficient that could be tracked was reduced from 4 μm^2/s in the single particle case (see Fig. 4) down to 0.4 μm^2/s. In Fig. 7 (bottom) we show the results when tracking three particles. The maximum diffusion coefficient was further reduced to 0.2 μm^2/s. In the absence of any stage dynamics, one would expect the tracking performance to scale inversely with the number of particles being tracked. When switching between particles, however, the stage needs to move a relatively long distance. The transient response of the stage thus plays a large role in the overall performance.

As seen in Fig. 2, the manufacturer's closed-loop controller has a cutoff frequency of approximately 300 Hz. To explore whether this is the limiting factor in the tracking performance, we ran the simulations using our controller which has a cutoff frequency of approximately 2 kHz. The sampling rate was set to 1 kHz. We first considered a single particle. The tracking error and standard deviation as a function of the diffusion constant are shown in Fig. 8 (top). The new low-level controller leads to slightly improved tracking performance with the maximum diffusion constant that can be tracked increasing from 4 μm^2/s to 5 μm^2/s. That only a small improvement was achieved is as expected since tracking a single particle does not require the large shifts needed in multiple particle tracking and thus the stage dynamics play a smaller role.

In Fig. 8 (bottom) we show the tracking error and standard deviation when tracking three particles. In this scenario,

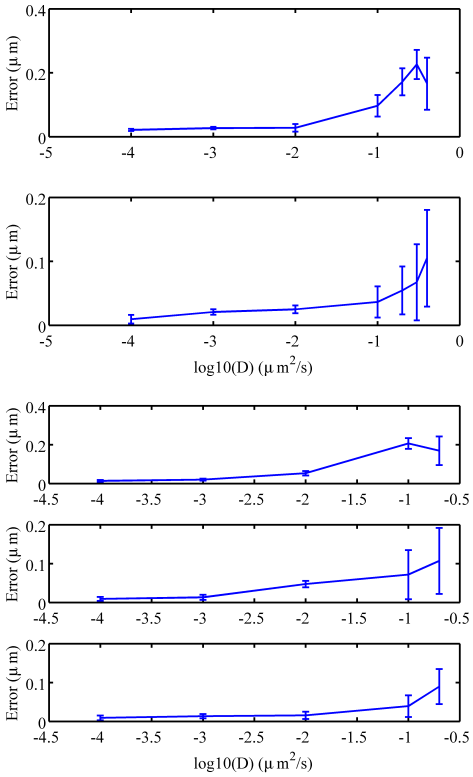

Fig. 7. Tracking error and std. dev. (error bars) as a function of the diffusion constant when tracking two (top) and three (bottom) particles. The max. diffusion coefficient for two particles was 0.4 μm^2/s while for three particles it fell to 0.2 μm^2/s.

tracking performance is greatly improved over the slower low-level controller with the maximum diffusion constant that can be tracked rising from 0.2 μm^2/s to 1.2 μm^2/s.

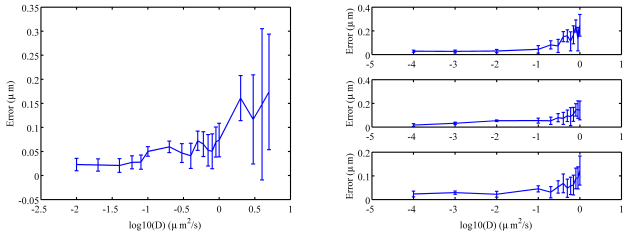

Fig. 8. Tracking error and std. dev. (error bars) as a function of the diffusion constant when tracking a single particle (top) and three particles (bottom) with the stage dynamics replaced by our higher-performance low-level controller. For one particle, performance is improved only slightly over the lower speed controller while in the multiple particle case an order-of-magnitude improvement in the tracking capability of the system is achieved.

V. Conclusions and Future Directions

In this paper, we introduced an LQG-based scheme for tracking multiple fluorescent particles in a confocal setup and explored its performance through numerical simulation. The simulation results provide guidance on choosing control parameters and indicate that the dynamics of the actuation stage play a large role when multiple particles are considered.

In addition to experimental implementation, we are considering three primary theoretical questions. First, the LQG system for the multiple particle case is a simple concatenation of LQG controllers for each particle independently. The combined system is thus suboptimal. We are seeking to improve upon these results by appealing to limited communication-based approaches [14]–[16]. Second, we are exploring better sampling patterns for the estimation procedure that take into account the dynamics of the stage as well as the noise characteristics of the estimator. Finally, we are extending the approach to tracking in three dimensions.

Acknowledgements

This work was supported in part by NSF through grant DBI-0649823.

References

[1] V. Levi, Q. Ruan, M. Plutz, A. S. Belmont, and E. Gratton, "Chromatin dynamics in interphase cells revealed by tracking in a two-photon excitation microscope," *Biophysical Journal*, vol. 89, no. 6, pp. 4275–4285, December 2005.

[2] F. Daumas, N. Destainville, C. Millot, A. Lopez, D. Dean, and L. Salomé, "Confined diffusion without fences of a G-protein-coupled receptor as revealed by single particle tracking," *Biophysical Journal*, vol. 84, no. 1, pp. 356–366, January 2003.

[3] M. Dahan, S. Lévi, C. Luccardini, P. Rostaing, B. Riveau, and A. Triller, "Diffusion dynamics of glycine receptors revealed by single-quantum dot tracking," *Science*, vol. 302, no. 5644, pp. 442–445, September 2003.

[4] A. J. Berglund and H. Mabuchi, "Feedback controller design for tracking a single fluorescent molecule," *Applied Physics B: Lasers and Optics*, vol. 78, no. 5, pp. 653–659, March 2004.

[5] S. B. Andersson, "Tracking a single fluorescent molecule with a confocal microscope," *Applied Physics B: Lasers and Optics*, vol. 80, no. 7, pp. 809–816, June 2005.

[6] V. Levi, Q. Ruan, and E. Gratton, "3-D particle tracking in a two-photon microscope: application to the study of molecular dynamics in cells," *Biophysical Journal*, vol. 88, no. 4, pp. 2919–2928, April 2005.

[7] S. B. Andersson and T. Sun, "Linear optimal control for tracking a single fluorescent particle in a confocal microscope," *Applied Physics B: Lasers and Optics*, vol. 94, no. 3, pp. 403–409, 2009.

[8] K. McHale, A. J. Berglund, and H. Mabuchi, "Quantum dot photon statistics measured by three-dimensional particle tracking," *Nano Letters*, vol. 7, no. 11, pp. 3535–3539, November 2007.

[9] J. Apgar, Y. Tseng, E. Fedorov, M. B. Herwig, S. C. Almo, and D. Wirtz, "Multiple-particle tracking measurements of heterogeneities in solutions of actin filaments and actin bundles," *Biophysical Journal*, vol. 79, no. 2, pp. 1095–1106, August 2000.

[10] J. Suh, M. Dawson, and J. Hanes, "Real-time multiple-particle tracking: applications to drug and gene delivery," *Advanced Drug Delivery Reviews*, vol. 57, no. 1, pp. 63–78, January 2005.

[11] S. B. Andersson, "Position estimation of fluorescent probes in a confocal microscope," in *Proceedings of the IEEE Conference on Decision and Control*, 2007, pp. 4950–4955.

[12] ——, "Localization of a fluorescent source without numerical fitting," *Optics Express*, vol. 16, no. 23, pp. 18 714–18 724, November 2008.

[13] D. Thomann, D. R. Rines, P. K. Sorger, and G. Danuser, "Automatic fluorescent tag detection in 3D with super-resolution: application to the analysis of chromosome movement," *Journal of Microscopy*, vol. 208, no. 1, pp. 49–64, October 2002.

[14] J. Baillieul and P. Antsaklis, "Control and communication challenges in networked real-time systems," *Proceedings of the IEEE*, vol. 95, no. 1, pp. 9–28, January 2007.

[15] L. Xie, W. Zhao, and Z. Ji, "LQG control of networked control system with long time delays using δ-operator," in *Proceedings of the Sixth International Conference on Intelligent Systems Design and Applications*, 2006, pp. 183–187.

[16] D. Hristu-Varsakelis and L. Zhang, "LQG control of networked control systems with access constraints and delays," *International Journal of Control*, vol. 81, no. 8, pp. 1266–1280, August 2008.